

Analysis of EEG networks and their correlation with cognitive impairment in preschool children with epilepsy

Eli Kinney-Lang^{a,b,*}, Michael Yoong^b, Matthew Hunter^b, Krishnaraya Kamath Tallur^c, Jay Shetty^c, Ailsa McLellan^c, Richard FM Chin^{†b,c}, Javier Escudero^{†a,b}

^a*School of Engineering, Institute for Digital Communications, The University of Edinburgh, Edinburgh EH9 3FB, United Kingdom*

^b*The Muir Maxwell Epilepsy Centre, The University of Edinburgh, Edinburgh EH8 9XD, United Kingdom*

^c*Royal Hospital for Sick Children, Edinburgh EH9 1LF, United Kingdom*

Abstract

Objective: Cognitive impairment (CI) is common in children with epilepsy and can have devastating effects on their quality of life and that of their family. Early identification of CI is a priority to improve outcomes, but the current gold standard of detection with psychometric assessment is resource intensive and not always available. This paper proposes a novel technique of network analysis using routine clinical electroencephalography (EEG) to help identify CI in children with early-onset epilepsy (CWEOE) (0-5 y.o.).

Methods: We analyzed functional networks from routinely acquired EEGs of 51 newly diagnosed CWEOE from a prospective population-based study. Combinations of connectivity metrics (e.g. phase-slope index (PSI)) with sub-network analysis (e.g. cluster-span threshold (CST)) identified significant correlations between network properties and cognition scores via rank correlation analysis with Kendall's τ . Predictive properties were investigated using a 5-fold cross-validated K -Nearest Neighbor classification model with normal cognition, mild/moderate CI and severe CI classes.

Results: Phase-dependent connectivity metrics had higher sensitivity to cognition scores, with sub-networks identifying significant functional network changes over a broad range of spectral frequencies. Approximately 70.5% of all children were appropriately classified as normal cognition, mild/moderate CI or severe CI using CST network features. CST classification predicted CI classes 55% better than chance, and reduced misclassification penalties by half.

Conclusions: CI in CWEOE can be detected with sensitivity at 85% (with respect to identifying either mild/moderate or severe CI) and specificity of 84%, by EEG network analysis.

*Corresponding author

† Authors contributed equally to the work.

Email address: e.kinney-lang@ed.ac.uk (Eli Kinney-Lang)

Significance: This study outlines a data-driven methodology for identifying candidate biomarkers of CI in CWEOE from network features. Following additional replication, the proposed method and its use of routinely acquired EEG forms an attractive proposition for supporting clinical assessment of CI.

Keywords: Network analysis, signal processing, EEG graph networks, paediatric epilepsy, developmental impairment

Highlights

- EEG network analysis correlates with CI in preschool children with epilepsy
- Classification reveals network features' predictive potential for CI identification
- Sensitivity to CI improves with dense networks and phase-based connectivity measures

1. Introduction

Epilepsy is a complex disease that can have devastating effects on quality of life [1]. Cognitive impairment (CI), which frequently and severely affects quality of life of children and their families, coexists in more than half of children with epilepsy [2, 3, 4, 5]. Timely identification of CI, particularly in children with early-onset epilepsy (CWEOE; epilepsy onset < 5 years of age) is critical because early-life interventions are likely to be more effective, it is the period in which childhood epilepsy is most common, and the most severe forms occur during this time [6, 7, 8]. An estimated 40% of CWEOE have CI [5]. The urgent need for emphasis on early recognition, novel interventions and improved public health strategies for primary and secondary prevention for CI in epilepsy is highlighted in calls to action by august bodies including the International League Against Epilepsy, The Institute of Medicine, and the World Health Organization [9, 10]. Therefore, there is a need to understand the causes of CI and find reliable, affordable and non-invasive markers beyond current standard approaches.

Identification of CI is especially difficult in CWEOE because the gold standard of diagnosis by psychological assessments may not be readily available [11], it is resource intensive, and can be clinically challenging (e.g. introducing potential bias from repeated testing) [11]. Thus, reliable, affordable and rapid CI screening techniques in clinical care are sought after. Such techniques would help focus further medical investigations and resources onto a smaller subgroup, producing efficiency gains and cost savings. Graph network analysis of standard routine clinical EEG recordings is one such potential technique.

Analysis of functional EEG networks offers a data-driven methodology for understanding diverse brain conditions through the lens of network (connec-

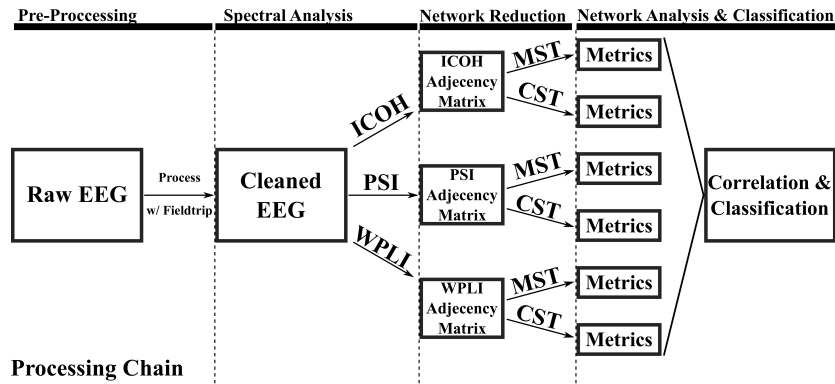


Figure 1: Flowchart of data processing chain for an individual child. ICOH = Imaginary part of coherency, PSI = Phase-slope index, WPLI = Weighted phase-lag index, MST = Minimum Spanning Tree, CST = Cluster-Span Threshold

27 tivity) properties [12, 13]. Functional networks examined as graphs are well-
 28 established, and provide advantages in understanding changes in connectivity
 29 across the brain, e.g. through exploiting properties like small-world topology,
 30 connected hubs and modularity [13]. Insights into epilepsy, including the sever-
 31 ity of cognitive disturbances, outcomes of epilepsy surgery, and disease duration
 32 have been found to correlate with the extent of changes in these functional net-
 33 works [14]. Recent work has also found network abnormalities can appear in
 34 both ictal and interictal states [14]. This supports that network can be distin-
 35 guished in resting-state EEG [14]. Therefore, functional graph analysis is well
 36 positioned as a potential tool to reveal insights into CI in CWEOE.

37 The aim of this study was to identify a reliable EEG network marker which
 38 could help effectively screen for CI in CWEOE. Our hypothesis was two-fold.
 39 First, informative network abnormalities could be revealed in CWEOE using
 40 graph network analysis on routine clinical EEGs. Second, identified abnormali-
 41 ties could be integrated into a simple machine learning paradigm to demonstrate
 42 predictive capabilities with respect to CI. We aimed to utilize a data-driven,
 43 quantitative approach to identify potential network markers. Then, we could
 44 integrate their information into a simple classification pipeline, which could be
 45 readily implemented to support clinical decisions regarding CI. By investigating
 46 only routine EEG recordings, we hoped to demonstrate that minimal potential
 47 cost and effort would be required to adopt our proposed technique in a clinical
 48 setting.

49 2. Methods

50 The data processing pipeline for each child is summarized in Figure 1.

51 *2.1. Dataset*

52 The details on study recruitment and assessments are reported elsewhere
53 [15]. In summary, newly diagnosed CWEOE of mixed epilepsy types and aetiolo-
54 gies were recruited as part of a prospective population-based study of neurode-
55 velopment in CWEOE. Parents gave approval for use of the standard, resting-
56 state, awake 10-20 EEG their child had as part of their routine clinical care. If a
57 child had multiple EEGs, only the first EEG was used to avoid biasing results to-
58 ward children with multiple recordings. Additionally, it allowed similar selection
59 of resting-state recordings across all children, e.g. awake resting-state. As such,
60 no EEG recordings of sleep were analysed in this work. All analyses were blinded
61 to any treatment or seizure frequency information. Participants underwent cog-
62 nitive assessment with age-appropriate standardized tools, e.g. Bayley Scales
63 of Infant and Toddler Development- Third Edition (Bayley-III) and Wechsler
64 Preschool and Primary Scale of Intelligence-Third Edition (WPPSI-III). Child-
65 ren who scored within ± 1 standard deviation (SD) of the normative mean
66 were defined as normal, -1 to -2 SD as having mild/moderate CI, and < -2
67 SD as having severe CI. The cognition scores from Bayley-III and WPPSI-III
68 tests were converted into a normalized standard score measure. Clinical details
69 were collected by members of the research team using a standardized proforma
70 by direct interview of care-givers, medical records and, where possible, patients
71 themselves when they attended for clinical and/or research study assessment.

72 Table 1 provides the demographic and clinical features for the CWEOE
73 which were included in this study. Given the broad anti-epileptic drug (AED)
74 therapies and aetiologies present in Table 1, potential interactions from AED
75 load or specific aetiology were examined with respect to the designated CI classes
76 (e.g. normal, mild/moderate, severe CI). Using a non-parametric version of the
77 two-way ANOVA (Friedman’s test [16]) on data from Table 1, we revealed no
78 significant interactions between any AED load or specific aetiology with respect
79 to any CI classes. This in turn suggests that the results identified via network
80 analysis are likely driven mainly by cognitive phenomena, as opposed to epileptic
81 syndrome or AED load effects.

82 A retrospective analysis was done on 32-channel, unipolar montage with
83 average reference captured routine EEGs. EEGs were recorded at 20 scalp
84 electrodes (FP1, FP2, FPz, F3, F4, F7, F8, Fz, C3, C4, Cz, P3, P4, Pz, T3,
85 T4, T5, T6, O1, O2), eight auxiliary electrodes (AUX1-8), two grounding (A1,
86 A2) and two ocular electrodes (PG1, PG2).

87 *2.2. Pre-processing*

88 EEG recordings were pre-processed in MATLAB using the Fieldtrip tool-
89 box [17]. The EEG had a sampling rate of approximately 511 Hz. Recordings
90 were re-referenced to a common average reference (CAR), and bandpass fil-
91 tered between 0.5-45 Hz in Fieldtrip. The resting-state data was split into non-
92 overlapping, two second long sub-trials; long enough to pick up any resting-state
93 network activity, while still fitting at least one full period of the lowest included
94 frequency.

	Normal ($n = 31$)	Mild/Moderate CI ($n = 7$)	Severe CI ($n = 13$)
Age in months (SD)	36.18 (19.87) [†]	26.76 (17.06)	20.37 (18.56) [†]
Male:Female Ratio	20:11	6:1	6:7
Ethnicity			
Asian	2 (6%)	–	1 (8%)
Black	–	1 (14%)	–
White (U.K./European)	29 (94%)	6 (86%)	12 (92%)
Antiepileptic Drugs			
None	3 (10%)	1 (14%)	–
Monotherapy	26 (84%)	6 (86%)	9 (69%)
Polytherapy	2 (6%)	–	4 (31%)
Focal Seizures	12 (39%)	3 (43%)	4 (31%)
Generalized Seizures	18 (58%)	2 (28%)	9 (69%)
Generalized and Focal	1 (3%)	2 (28.5%)	–
Epilepsy aetiology			
Cryptogenic	3 (10%)	1 (14%)	5 (38%)
Idiopathic	24 (77%)	4 (57%)	1 (8%)
Symptomatic	3 (10%)	2 (29%)	7 (54%)
Unknown	1 (3%)	–	–
Cognitive z -score (SD)	-0.05 (0.66)	-1.41 (0.20)	-2.9 (0.27)

Table 1: Demographic and clinical feature information of patients, grouped by CI classes of normal, mild/moderate CI, and severe CI. Significant differences between groups with respect to age are indicated by a [†] (Kruskal-Wallis with post-hoc Mann-Whitney U; $H = 6.4697$, $p < 0.05$, with mean ranks of 30, 23.7143, and 17.6923 for Normal, Mild/Moderate CI and Severe CI respectively.)

95 Prior to data processing, seizure activity in the EEGs were confirmed by
96 clinicians. Whole trials which contained seizure activity were excluded from
97 the analysis, rather than excluding only sections of trials with evident seizure
98 activity. This helped guarantee that all network trials were derived from a
99 minimum of two continuous seconds of seizure-free EEG. The small time window
100 helped to balance removing large amounts of useful EEG data, while retaining
101 enough data to characterize the frequencies present.

102 Standard EEG artefacts were rejected using a 2-step approach with manual
103 and automatic rejection. Manual artefact rejection first removed clear outliers
104 in both trial and channel data based upon high variance values ($var > 10^6$).
105 Muscle, jump and ocular artefacts were then automatically identified using strict
106 rejection criteria relative to the Fieldtrip default suggested values [17] (Field-
107 trip release range R2015-R2016b, z -value rejection level $r = 0.4$). All trials
108 containing EEG artefacts were excluded from analysis. For subjects, we aver-
109 aged across all trials at each frequency band, to help reduce potential bias and
110 variance resulting from our selection of a shorter analysis window.

111 A narrow band (2-Hz wide) approach was used in analysis of clean EEG
112 data, similar to work done by Miskovic et al. [18]. Segmenting the frequency
113 range into these narrow bands (e.g. 1-3 Hz, 3-5 Hz,...) provided a data-driven
114 approach to interrogate networks across subjects. The a priori nature of the in-
115 vestigation avoided attempts at equivocating the (likely heterogeneous) impact
116 of epilepsy, development, medication etc. on each child’s spectral EEG compo-
117 sition. While such narrow bands may eschew some physiological interpretations

118 by not adhering to classical frequency bands, the narrow bands promoted iden-
119 tification of mainly robust, common network abnormalities across the heteroge-
120 neous CWEOE population. If significant network abnormalities were identified
121 in these narrow frequency bands (after correction for multiple comparisons, age
122 and spurious correlations) then the identified results were likely a strong effect.

123 *2.3. Network Coupling Analysis*

124 The processed data was analyzed using functional EEG graph analysis, based
125 on ‘functional links’ connecting any pair of EEG channels i and j , derived from
126 the cross-spectrum of the data. Appendix A provides the detailed, formal def-
127 initions for the cross-spectrum and the network analysis methods described
128 below. A summary of these definitions are included here for clarity. In brief,
129 this study selected several measures of dependencies in EEG recordings, cre-
130 ated graph networks based on these measures and characterized the created
131 networks to identify candidate biomarkers for classification and identification of
132 CI in CWEOE.

133 This study investigates three connectivity analysis methods building from
134 the cross-spectrum viz: (1) the imaginary part of coherency (ICOH) [19], (2)
135 phase-slope index (PSI) [20], and (3) weighted phase-lag index [21, 22].

136 ICOH is a standard measure in functional network analysis [19]. ICOH is
137 well documented, and has been shown to provide direct measures of true brain
138 interactions from EEG while eliminating self-interaction and volume conduction
139 effects [19]. A weakness of ICOH, however, is its dependence on phase-delays,
140 resulting in identifying functional connections only at specific phase differences
141 between signals, while completely failing for others [21, 22, 23].

142 The PSI [20] was selected as a complementary alternative to ICOH for anal-
143 ysis. In practice, the PSI examines causal relations (temporal order) between
144 two sources for signals of interest, e.g. s_i and s_j [20]. PSI exploits the phase
145 differences between the sources to identify the ‘driving’ versus ‘receiving’ re-
146 lationship between the sources [20]. Their average phase-slope differences are
147 used to identify functional links [20]. Importantly, unlike ICOH, the PSI is
148 equally sensitive to all phase differences from cross-spectral data [20]. However,
149 the PSI equally weights contributions from all phase differences, meaning even
150 small phasic perturbations are equal to the (defining) large perturbations.

151 Therefore the weighted phase-lag index (WPLI) was included as a third compar-
152 ative measurement for analysis [21, 22]. The standard phase-lag index (PLI)
153 [21] is a robust measure derived from the asymmetry of instantaneous phase
154 differences between two signals, resulting in a measure which is less sensitive to
155 volume conduction effects and independent of signal amplitudes [21]. The PLI
156 ranges between 0 and 1, where PLI of zero indicates no coupling (or coupling
157 with a specific phase difference; see [21] for details), while a PLI of 1 indicates
158 perfect phase locking [21]. The PLI’s sensitivity to noise, however, is hindered
159 as small perturbations can turn phase lags into leads and vice versa [22].

160 A weighted version of the PLI was introduced (weighted PLI; WPLI) [22]
161 to counter this effect. The WPLI adds proportional weighting based on the

162 imaginary component of the cross-spectrum [22]. The proportional weighting
163 alleviates the noise sensitivity in PLI. The WPLI, like the PSI, helps capture
164 potential phase-sensitive connections present in EEG networks from another
165 perspective.

166 *2.4. Adjacency Matrices and Sub-Networks*

167 The estimated functional connectivity between channel pairs i and j com-
168 prising the weighted functional network of a subject can be represented by an
169 adjacency matrix. The functional connections found for the ICOH, PSI, and
170 WPLI measures were therefore represented via adjacency matrices in the analy-
171 sis below. A set of adjacency matrices for a representative normal and impaired
172 cognition child in the range of 5-9 Hz are included in Appendix B, Figures B.5
173 and B.6, respectively.

174 Methodological choices associated with constructing and comparing graphs
175 from the adjacency matrix can introduce bias in the network analysis (see [24,
176 25, 26] for details). Therefore, we used two methods for defining unbiased sub-
177 networks of the functional EEG for comparison and analysis: the Minimum
178 Spanning Tree (MST) [24] and the Cluster-Span Threshold (CST) [27].

179 The MST is an acyclic, sub-network graph which connects all nodes (elec-
180 trodes) of a graph while minimizing link weights (connectivity strength) based
181 on applying Kruskal's algorithm on the weighted network [24, 28]. In brief, the
182 algorithm orders the link weights in a descending manner (i.e. from strongest
183 connection to weakest), constructing the MST by starting with the largest link
184 weight and adding the next largest link weight until all nodes, N , are connected
185 in an acyclic sub-network with a fixed density of $M = N - 1$ [24]. After con-
186 struction of the sub-network, all weights are assigned a value of one [24]. In this
187 manner, the MST is able to efficiently capture a majority of essential properties
188 underlying a complex network in an unbiased sub-network [24].

189 Exploiting the properties of the MST is a standard technique common in
190 recent publications exploring brain networks [24]. However, since the MST
191 naturally leads to sparse networks in the data due to its acyclic nature, and that
192 in some occasions more dense networks may be preferable, there is potentially
193 real brain network information lost in the MST based EEG graph analysis [29].

194 By contrast, the CST creates a similar sub-network, but balances the pro-
195 portion of cyclic 'clustering' (connected) and acyclic 'spanning' (unconnected)
196 structures within a graph (for details see [27]). This balance thus retains nat-
197 urally occurring 'loops' which can reflect dense networks without potential in-
198 formation loss [29] while still producing an unbiased sub-network for analysis.
199 Figure 2 illustrates a topographical example of EEG channels connected via
200 MST and CST networks for a randomly selected child. Differences in sparsity
201 between the acyclic MST and the cyclic CST sub-networks can readily be seen
202 in Figure 2. Both the MST and CST are binary sub-networks, which have addi-
203 tional advantages over weighted networks, e.g. the adjacency matrix [24, 27, 29].

204 For each combination of sub-networks and connectivity definitions above
205 (e.g. MST-ICOH, CST-ICOH, MST-PSI, etc.) four network metrics were in-
206 vestigated for correlation to the cognition standard score measures. To help

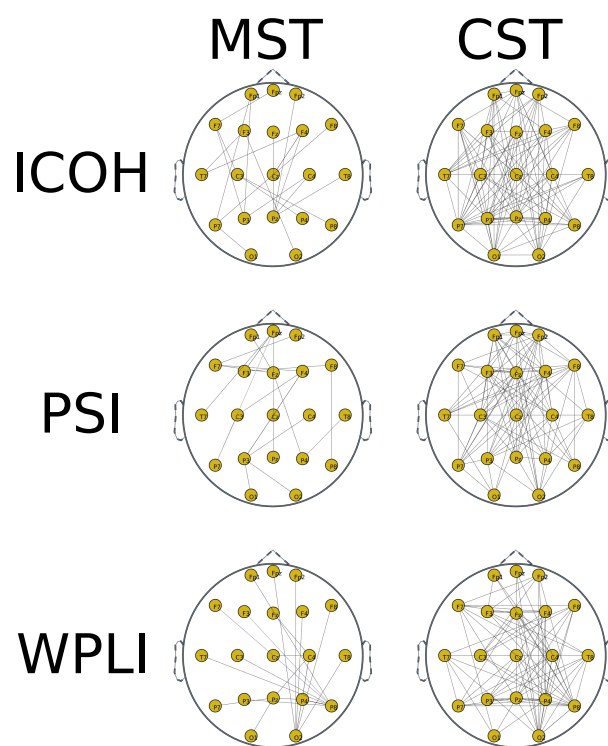


Figure 2: Illustrative examples of the MST and CST sub-network graphs of ICOH, PSI and WPLI for a randomly selected child. EEG channels are displayed as nodes, with functional connections displayed for each combination of sub-network and connectivity measure.

207 reduce potential selection bias, network metrics for analysis were agreed upon a
208 priori. Metrics were chosen to account for distinct network properties (e.g. the
209 shape of the network, the critical connection points in the network etc.) with
210 (relatively) little inter-correlation. Due to the natural exclusion/inclusion of cy-
211 cles, the network metrics differ for the MST and CST, respectively. However, all
212 metrics across sub-networks were selected to be comparable regarding network
213 properties. Pictorial examples of the selected network metrics, alongside short
214 definitions, are outlined in Figure 3.

215 *2.5. Statistical Analysis*

216 Statistical analysis was done using Matlab 2015a. Correlation between in-
217 dividual network metrics and the cognition standard score was measured using
218 Kendall’s tau (τ) [30]. Kendall’s τ calculates the difference between concor-
219 dant and discordant pairs [30, 31], and is ideal for describing ordinal or ranking
220 properties, like the normalized cognition standard score. Its design is also rela-
221 tively robust to false positive correlations from data outliers [30, 31], providing
222 additional mitigation to spurious correlations in the results. Furthermore, as
223 Kendall’s τ is a non-parametric hypothesis test it did not rely on any underly-
224 ing assumptions about the distribution of the data. Therefore our correlation
225 analysis was robust to any potential ceiling, floor or skewed distribution effects
226 present in the reported cognition standard score measures.

227 Correlation trends are reported both as uncorrected $p < 0.05$ values, and
228 with multiple comparison (Bonferroni) corrections, similar in style to previous
229 literature [32]. For each frequency bin (2-Hz wide) and network, we compared
230 and corrected for the 4 separate graph measures using the Bonferroni technique
231 (i.e. we set $p = 0.05/4 = 0.0125$ as the threshold for significance). Dependency
232 was assumed across the small 2-Hz frequency bins, similar in principle to [32],
233 and as such we do not include the frequency bins in the Bonferroni correction.
234 Correlations which are found to be potentially significant under this assumption
235 are indicated by the † symbol for Bonferroni corrections.

236 *2.6. Classification*

237 A multi-class classification scheme was devised using the Weka toolbox [33,
238 34]. Class labels of *normal*, *mild/moderate CI*, and *severe CI* were applied.

239 Primary feature selection included all correlations identified by the statistical
240 analysis, thereby allowing potential interpretation of the retained network fea-
241 tures. Then, a second feature selection phase using nested 5-fold cross-validation
242 selected prominent features via bi-directional subspace evaluation [35]. Within
243 this nested cross-validation, features identified as important in $> 70\%$ of the
244 folds were selected for use in classification.

245 Due to natural skew of the data (towards normalcy), and the context of
246 the classification problem (e.g. misclassifying different classes has various im-
247 plications), a cost-sensitive classifier was developed [36]. In order to properly
248 develop such a classifier, an appropriate cost matrix needed to be identified.

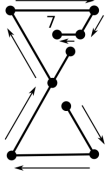
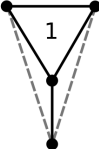
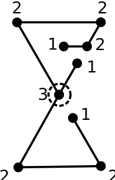
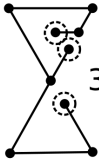
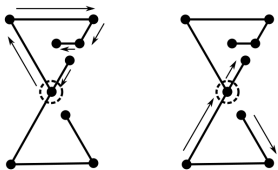
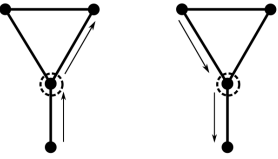
MST	CST
<p>Diameter: The longest 'shortest path' from any two nodes</p>  <p>= 7</p>	<p>Clustering Coefficient: Formed 'clustering' triangles out of all possible triangle clusters (max)</p>  <p>= 1/4</p>
<p>Max Degree: The node with the largest number of connecting edges</p>  <p>= 3</p>	<p>Average Degree: The average degree of all graph nodes</p>  <p>= 2</p>
<p>Leaf Fraction: The fraction of the total nodes with degree = 1</p>  <p>3/9 = 1/3</p>	<p>Variance Degree: The variance of all degree values in a graph</p>  <p>= 1/2</p>
<p>Betweenness Centrality: Measures 'centrality' of nodes with respect to various shortest paths</p> 	<p>Betweenness Centrality: Measures 'centrality' of nodes with respect to various shortest paths</p> 

Figure 3: Illustration of all graph analysis metrics for the Minimum Spanning Tree (MST) and Cluster-Span Threshold (CST) networks using simple example graphs. Nodes (dots) represent EEG channel electrodes. Edges (lines) represent functional interactions between EEG channels identified by a connectivity measure, e.g. ICOH/PSI/WPLI.

Multi-class Classification Cost Matrix

		CI-Predicted Class		
		Normal	Mild/Mod.	Severe
CI-True Class	Normal	0	2.5	2.5
	Mild/Mod.	5	0	1
	Severe	5	1	0

Table 2: Weighted cost matrix for misclassification of cognitive impairment (CI) for normal (± 1 SD), mild/moderate (-1 to -2 SD) and severe (< -2 SD) classes. Rows represent true class labels, with columns as the predicted classification labels.

249 Using guidelines outlined in literature [36], the cost matrix in Table 2 was de-
 250 veloped, with predicted classes on the rows and real classes on the columns.

251

252 The defined matrix satisfies several key concerns in multi-class cost-matrix
 253 development [36]. The weights on misclassification were carefully selected to
 254 reflect probable clinical concerns in classification with guidance from paediatric
 255 neurologists (RC, JS). The cost for incorrectly classifying an impaired child
 256 as normal was twice as heavy compared to misclassifying a normal child into
 257 either impaired group, which was still significantly more punishing than cor-
 258 rectly identifying impairment and only misclassifying between mild/moderate
 259 or severe impairments. These weighted values prioritized correctly including as
 260 many ‘true positive’ CWEOE with CI, i.e. increasing sensitivity, followed by a
 261 secondary prioritization upon being able to discern the level of CI. These bound-
 262 aries provide a more clinically relevant classification context in the analysis.

263 Using the selected features and developed cost-sensitive matrix, a nested
 264 5-fold cross-validation trained a simple K -Nearest Neighbour (KNN) classifier,
 265 with $N = 3$ neighbours and Euclidean distance to minimize the above costs.
 266 By demonstrating our proof-of-concept results with a simple classifier first, e.g.
 267 KNN, we aimed to highlight that network response found from our analysis
 268 pipeline was likely robust. A repeated ‘bagging’ (Bootstrap Aggregation [37])
 269 approach was used to reduce variance in the classifier at a rate of 100 iter-
 270 ations/fold. Results were evaluated upon their overall classification accuracy
 271 and total penalty costs (e.g. sum of all mistakes based on the cost matrix).

272 Random classification and naive classification (e.g. only choosing a single
 273 class for all subjects) were included for comparison. In this study, random clas-
 274 sification refers to classification of any ‘true’ class label to a randomly selected
 275 ‘predicted’ class label. Based on the distribution of subjects into the classes, a
 276 ‘chance’ level for each class is used to assign the ‘predicted’ label at random.
 277 Naive classification (e.g. single-class classification), assumes that all subjects
 278 belong to only one class. Classification accuracy and misclassification penalties
 279 are then calculated based on the presumed (single) class assignment. This study
 280 looked at naive classification for each class label, and have reported comparisons
 281 to each possible naive classification.

282 3. Results

283 Of 64 children enrolled into the parent study, 13 were excluded from the
284 current study due to corrupted EEG data and inconsistent or incompatible EEG
285 acquisition parameters. There were data available for analysis on 51 children
286 (32:19 male-to-female ratio, mean age and SD of 30.85 ± 20.08 months). On
287 average approximately 455 ± 325 two second trials were used for each child in
288 the analysis, totalling 15.16 ± 11.87 minutes of resting-state EEG data for each
289 child. Thirty-one children had normal cognition, 7 had mild/moderate CI, and
290 13 had severe CI.

291 3.1. Correlation Analysis

292 Each combination of functional link analysis (ICOH/PSI/WPLI) and sub-
293 network selection (MST/CST) techniques uncovered likely correlations between
294 at least one network metric (outlined in Figure 3) and the cognition standard
295 score measures. A summary of the significant correlations between the MST
296 metrics and the standard scores are shown in Table 3. All MST correlations
297 were in the medium to high frequency range, 9 – 31 Hz, with no significant
298 results in lower frequencies. Activity above approximately 9 Hz is outside of the
299 expected range for the delta, theta and alpha bands in young children [38, 39].
300 Sets of contiguous frequency bands with significant correlations were found in
301 the ICOH and PSI connectivity measures, and are reported together as a single
302 frequency range. Overlapping correlations retained at significant levels after
303 partial correlation correcting for age are also reported for the MST using a
304 modified Kendall’s τ .

305 Similarly, significant correlations between the CST metrics and the cogni-
306 tion standard scores are shown in Table 4. Several significant CST metrics exist
307 in the lower frequency range (< 9 Hz), indicating a potential sensitivity of the
308 CST to lower frequencies. No sets of continuous frequency bands were discov-
309 ered, but several sets were trending towards this phenomenon within ICOH.
310 Multiple overlapping correlations remaining after partial correlation correction
311 for age from the modified τ in the CST at lower frequencies indicate additional
312 sensitivity.

313 Both the MST and CST demonstrate high sensitivity in the phase-dependent
314 measures (PSI, WPLI) compared to the standard ICOH.

315 3.2. KNN Classification

316 Based upon CST’s sensitivity, a preliminary classification scheme assessed
317 the potential predictive qualities of the CST network metrics in identifying CI
318 classes. The relative quality of the classifications are examined using classifica-
319 tion accuracy and total ‘cost’ (i.e. penalty for misidentification) [36].

320 The subset of CST metrics for classification, identified from significant cor-
321 relations and chosen via cross-validated feature selection, included five network
322 metrics across the three connectivity measures. For ICOH, the identified subset
323 selected was the betweenness centrality at ranges 11-13 and 19-21 Hz along-
324 side the clustering coefficient at a range of 15-17 Hz. The subset also included

MST analysis of cognition standard score measures			
Network Type	Network Measurement	Frequency Range(s) (Hz)	Correlation ($\bar{\tau} \pm SD$)
ICOH	Diameter	–	–
ICOH	Maximum Degree	–	–
ICOH	Leaf Fraction	–	–
ICOH	Betweenness Centrality	13-17 Hz	-0.231 ± 0.001
PSI	Diameter	9-19 Hz	$0.239 \pm 0.032^{\dagger*}$
PSI	Maximum Degree	11-13 Hz	$-0.232 \pm 0.000^*$
PSI	Maximum Degree	15-17 Hz	$-0.258 \pm 0.000^{\dagger*}$
PSI	Maximum Degree	21-23 Hz	-0.219 ± 0.000
PSI	Leaf Fraction	11-13 Hz	-0.201 ± 0.000
PSI	Leaf Fraction	15-19 Hz	-0.246 ± 0.003
PSI	Betweenness Centrality	9-13 Hz	$-0.218 \pm 0.012^*$
PSI	Betweenness Centrality	17-19 Hz	$-0.259 \pm 0.000^{\dagger*}$
WPLI	Diameter	–	–
WPLI	Maximum Degree	29-31 Hz	$-0.310 \pm 0.000^{\dagger*}$
WPLI	Leaf Fraction	–	–
WPLI	Betweenness Centrality	23-25 Hz	0.223 ± 0.000

Table 3: Summary of Kendall’s τ correlation trends between various graph metrics and the cognition standard scores using the Minimum Spanning Tree (MST). For all values $|\tau|$ was between 0.201 and 0.310; mean = 0.239 ± 0.0278 and uncorrected $p < 0.05$. Significant values across contiguous narrow-band frequencies have been grouped together for ease of interpretation.

[†] Significant with Bonferroni correction at the level of frequencies.

* Significant after partial correlation correction to age of subjects, via modified τ with uncorrected $p < 0.05$.

325 the PSI average degree at 13-15 Hz and the WPLI variance degree from 1-3
 326 Hz. These results indicate specifically which network metrics, from a machine-
 327 learning perspective, contributed the most information for building an accurate
 328 classification model. As such, the classifier was trained specifically, and only,
 329 using these 5 key metrics. An illustrative example of these 5 selected network
 330 metrics (e.g. features) are shown in Figure 4 as scatter plots. When training
 331 the classifier, these network features are used to identify the underlying patterns
 332 not readily observed, and are incorporated into guiding the machine learning
 333 algorithm.

334 It bears repeating that Kendall’s τ is a non-parametric significance test,
 335 which means it does not rely on an underlying assumption of a specific type of
 336 distribution in the data. Therefore, Kendall’s τ correlation was robust to the
 337 apparent flooring effect seen in the severe CI class, as it utilizes concordant and
 338 discordant pairs. Therefore our choice of features from the statistical analysis
 339 remains unaffected.

340 The resulting confusion matrix from the 5-fold cross-validated, cost-sensitive
 341 classification analysis is seen in Table 5, with key summary

342 The overall classification accuracy was defined as the number of true label
 343 classes correctly predicted by the classifier, e.g. the true positive diagonal of
 344 Table 5. Presently, approximately 36 of the 51 children’s cognitive class (e.g.
 345 normal, mild/moderate CI, severe CI) were correctly predicted, giving a total
 346 accuracy of the classifier at 70.6%. Using Table 2, an overall ‘cost-penalty’ value

CST analysis of cognition standard score measures			
Network Type	Network Measurement	Frequency Range(s) (Hz)	Correlation ($\bar{\tau} \pm SD$)
ICOH	Clustering Coefficient	15-17 Hz	$-0.290 \pm 0.000^{\dagger*}$
ICOH	Average Degree	–	–
ICOH	Variance of Degree	13-15 Hz	-0.200 ± 0.000
ICOH	Variance of Degree	21-23 Hz	-0.203 ± 0.000
ICOH	Betweenness Centrality	11-13 Hz	$-0.273 \pm 0.000^{\dagger*}$
ICOH	Betweenness Centrality	15-17 Hz	-0.241 ± 0.000
ICOH	Betweenness Centrality	19-21 Hz	-0.203 ± 0.000
PSI	Clustering Coefficient	–	–
PSI	Average Degree	13-15 Hz	-0.210 ± 0.000
PSI	Variance of Degree	15-17 Hz	$-0.277 \pm 0.000^{\dagger*}$
PSI	Variance of Degree	21-23 Hz	-0.217 ± 0.000
PSI	Betweenness Centrality	5-7 Hz	$0.204 \pm 0.000^*$
PSI	Betweenness Centrality	15-17 Hz	-0.248 ± 0.000
WPLI	Clustering Coefficient	1-3 Hz	$-0.236 \pm 0.000^*$
WPLI	Clustering Coefficient	17-19 Hz	$0.287 \pm 0.000^{\dagger*}$
WPLI	Average Degree	–	–
WPLI	Variance of Degree	1-3 Hz	$-0.236 \pm 0.000^*$
WPLI	Betweenness Centrality	–	–

Table 4: Summary of Kendall’s τ correlation trends between various graph metrics and the cognition standard scores using the Cluster-Span Threshold (CST). For all values $|\tau|$ was between 0.201 and 0.290; mean = 0.237 ± 0.033 , and uncorrected $p < 0.05$. Significant values across contiguous narrow-band frequencies have been grouped together for ease of interpretation.

[†] Significant with Bonferroni correction at the level of frequencies.

* Significant after partial correlation correction to age of subjects, via modified τ with uncorrected $p < 0.05$.

Confusion Matrix from Classification Results

		CI-Predicted Class		
		Normal	Mild/Mod.	Severe
CI-True Class	Normal	26	<i>2</i>	<i>3</i>
	Mild/Mod.	2	3	<i>2</i>
	Severe	1	<i>5</i>	7

Table 5: Resulting confusion matrix from the 5-fold cross-validated, cost-sensitive classification scheme for all $n = 51$ children based on costs in Table 2. Rows represent true class labels, with columns as the predicted labels from the classification. Bold values along the diagonal show true positive classification results, where actual and predicted cognitive classes were accurately identified. Italicized values indicate children predicted to have CI, i.e. mild/moderate or severe class, by the classification scheme.

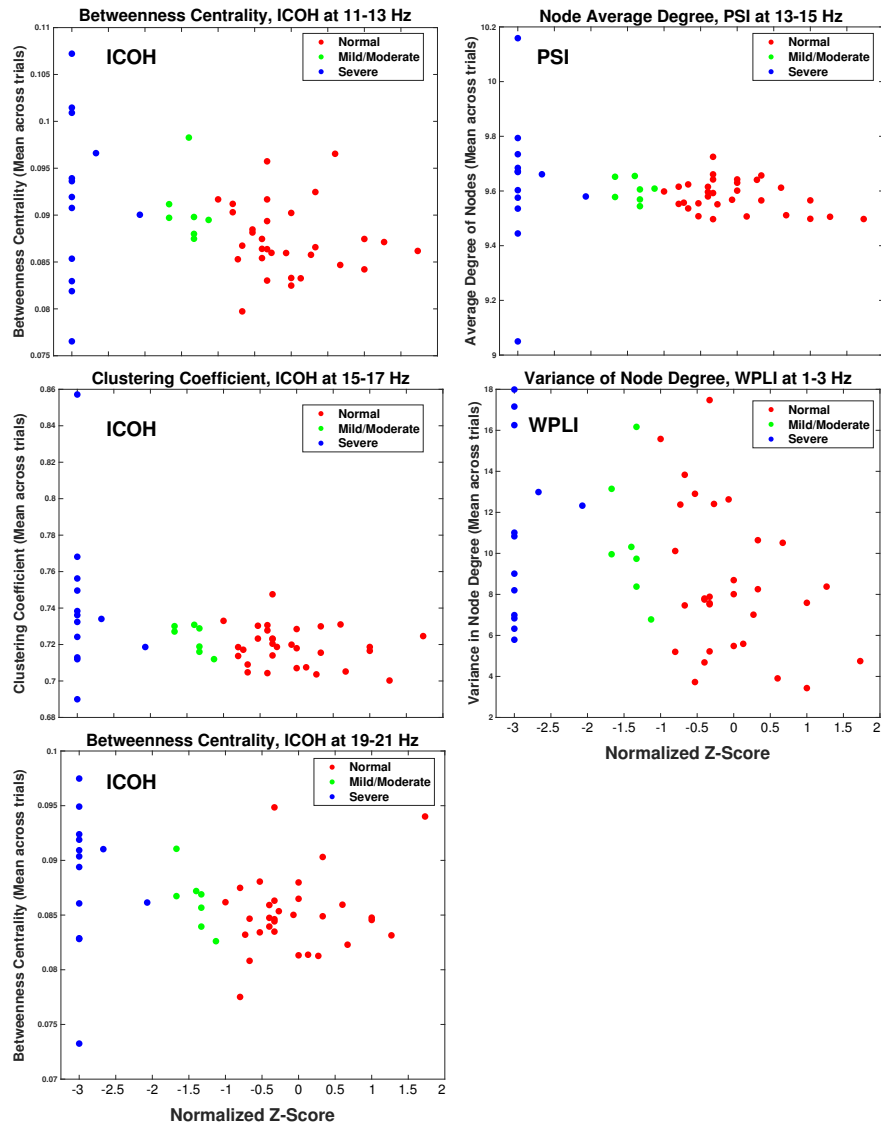


Figure 4: Scatter plot displaying the distribution of children for each of the 5 features used in training the KNN classification. Each panel displays network values on the y-axis, with the normalized cognition standard score (z-score) on the x-axis. Children classified into normal, mild/moderate CI and severe CI classes are displayed in red, green and blue respectively.

	Classification Scheme			
	Network Analysis	Random	Naive Class	Naive Value
Total Accuracy	70.6% (36/51)	45.4%(\approx 23/51)	Normal Cognition Mild/Moderate CI Severe CI	60.8% (31/51) 13.7% (7/51) 25.5% (13/51)
Total Cost Penalty	38 pts	\approx 65 pts	Normal Cognition Mild/Moderate CI Severe CI	100 pts 90.5 pts 84.5 pts

Table 6: Summary table of overall classification accuracies and total cost penalty for the proposed network analysis, random classification, and naive (single class) classification. Naive classification is split to show overall classification accuracy and cost penalties if all children were assigned as normal cognition, mild/moderate CI or severe CI classes. Total accuracy includes the approximate number of children with true positive predictions, out of total number of children evaluated.

347 was calculated at 38 points, based on the children who were misclassified, i.e.
348 their cognitive class was not correctly predicted.

349 The expected random classification accuracy is based on the distribution
350 of individuals belonging to each class, i.e. 31, 7 and 13 children for the *nor-*
351 *mal*, *mild/moderate* and *severe* classes respectively. Random accuracy would
352 be expected at 45.4%, with cost-penalty varying depending on misclassification
353 distributions. Using the average misclassification penalty and the percentage of
354 misidentified children (approximately 28 of the 51 subjects), the cost-penalty
355 would be at least 65 points.

356 Naive, or one-class classification assumes all subjects belong to a single class
357 only. For example, if all children were considered to only belong to the ‘normal’
358 cognition class (i.e. naively classified as normal), then exactly 31 of the 51
359 children (those whose true class is ‘normal’-the first row of Table 5) would be
360 correctly identified, giving a naive classification accuracy of 60.8%. Repeating
361 this naive classification scheme for mild/moderate and severe classes provides
362 naive classification accuracies of 13.7% (7/51), and 25.5% (13/51) respectively.
363 Similarly, the total cost-penalty for each naive classification would be 100, 90.5
364 and 84.5 points respectively, using the same procedure and the penalty costs
365 from Table 2.

366 Overall, the results indicate gains in classification accuracy and a reduced
367 total penalty as compared to both random and naive classification. This is
368 summarized in Table 6.

369 4. Discussion

370 The main finding of this study is the development of novel methods towards
371 identifying a potential computational biomarker for CI in CWEOE. The auto-
372 mated and quantitative nature of the processing chain, ability to appropriately
373 predict CI classes, and its use of routinely acquired EEG data make the pro-
374 posed methods an attractive proposition for clinical applications. Our results
375 indicate a substantial pool of potential characteristics might be identified using
376 the proposed methods with several network analysis and filtering combinations.

377 The breadth of these combinations emphasizes the general suitability of EEG
378 networks in identifying possible CI markers in CWEOE.

379 Flexibility in sensitivity and robustness of particular networks to features
380 of interest is an advantage of this analysis. For instance, the sensitivity of
381 phase-dependent connectivity measures, e.g. PSI and WPLI, was more preva-
382 lent compared to standard ICOH. This is not surprising as phase-oriented mea-
383 sures were developed to improve upon phase ambiguities in traditional ICOH
384 measurements [20, 23]. In addition, the sensitivity of PSI in picking up signifi-
385 cant correlations can be attributed in part to its equal treatment of small phase
386 differences in leading and lagging signals [20]. Such small phase differences con-
387 tribute equally in PSI, while counting for proportionally less in the WPLI by
388 definition [22, 21]. By construction, the WPLI results are substantially more
389 robust to noise and small perturbations in phase, through proportionally reflect-
390 ing phase differences in network connections with appropriate weights, providing
391 results for only large phase differences. Together these measures reflect trade-off
392 choices between sensitivity and robustness for network analysis.

393 Of interest for paediatric populations is the CST’s capability to identify low
394 frequency correlations in phase-dependent coherency measures. Both the PSI
395 and WPLI demonstrate sensitivity to lower frequencies, not present in the ICOH
396 or MST in general. This is critical considering that in preschool children lower
397 frequencies typically contain the bands of interest present in adult EEGs, e.g.
398 the delta/theta/alpha bands [38, 39]. During development these bands shift to
399 higher frequencies [40], reflecting a large scale reorganization of the endogenous
400 brain electric fields and suggesting a transition to more functionally integrated
401 and coordinated neuronal activity [18]. The (low) chance of all such significant
402 findings being spurious is of less detriment than the potential loss of impact
403 for disregarding the findings if at least one of them is true. The sensitivity to
404 detect network disruptions already present in these critical bands in CWEOE
405 provide high value in adjusting potential therapeutic and treatment strategies
406 for clinicians.

407 The identified subset of metrics for classification provide additional informa-
408 tion. All of the features in the subset reflected distribution measures of hub-like
409 network structures in the brain, relating to the balance between heterogene-
410 ity and centrality within the network. The implicated metrics, other than the
411 variance degree, corresponded to measures identifying local, centralized ‘criti-
412 cal’ nodes in a network. Their negative correlation to the cognition standard
413 scores imply that children with more locally centralized brain networks, and
414 consequently with less well distributed hub-like structures, are more likely to
415 have corresponding cognitive impairment. This is reasonable, since if there ex-
416 ists a small set of central, critical hubs responsible for communication across the
417 brain, disruption of these critical points (e.g. due to seizure activity) would have
418 severely negative effects on communication connections. This is also supported
419 by the negative correlation in the variance degree metric in the WPLI. The vari-
420 ance degree can be interpreted as a measure of a network’s heterogeneity [41].
421 As such, the negative variance degree in the low (1-3 Hz) frequency range may
422 reflect stunted cognitive development, as normal maturation is associated with

423 reduced activation in low frequencies [42, 38, 43, 39, 44], implying a decrease
424 in local connectivity and heterogeneity of the networks. This compliments the
425 above conclusions, suggesting a sensitivity in the likely well-centralized networks
426 to significant disruptions by epilepsy. The disrupted networks may then be re-
427 flected by the continued heterogeneity and local connectivity of low frequency
428 structures in impaired children.

429 Being able to predict the likely extent of CI using the identified markers could
430 provide an advantageous tool for clinicians. Specifically, being able to pair spe-
431 cific network features to an effective prediction of CI would allow clinicians to
432 retain the interpretability of the chosen network features while providing a tool
433 to quickly and objectively separate similar cases. To this end, the cost-sensitive,
434 simple KNN classifier explored in this work illustrates an early step towards
435 this aim. Evaluating the network-based classifier results show the analysis was
436 successful at two levels. First, the proposed classifier was able to generally
437 identify cognitively normal children from impaired children, when grouping the
438 mild/moderate CI and severe CI classes. This is seen in the first column of
439 Table 5 where only three impaired children are misidentified as ‘normal cogni-
440 tion’, giving a sensitivity of 85%. In other words, 17 of the 20 actual impaired
441 children were correctly identified as belonging to either the mild/moderate or
442 severe CI classes, demonstrating that the proposed network analysis and clas-
443 sifier was largely successful with respect to predicting children with some form
444 of impaired cognition, based on using the standard score definition. Similarly,
445 only five normal children were misidentified as generally impaired (i.e. classified
446 to either the mild/moderate or severe CI classes; top row of Table 5), giving a
447 specificity of approximately 84% (26/31) for appropriately identifying children
448 in the range of normal cognition. In addition, the network coupled classifier
449 was able to separate out cases of mild/moderate impairment from severe im-
450 pairment decently, with $> 50\%$ of impaired children correctly predicted. Thus,
451 the proposed classifier and associated methods provide considerable sensitivity
452 (85%) and specificity (84%) for clinicians in determining potential CI, while still
453 remaining relatively accurate in separating CI according to severity.

454 Statistical analysis in this manuscript was utilized as a first-pass means to
455 reduce the potential feature space for classification. Through identifying po-
456 tentially significant networks of interest, the number of features to test in the
457 classification step was substantially reduced. Through the statistical filter, we
458 were able to select pertinent features from a relevant and manageable feature
459 space. Future endeavours could refine such features, based on different choices
460 for the statistical analysis. Using a more rigid/flexible analysis could lead to
461 further culling/relaxation of the feature space and provide an adjustable frame-
462 work for examining network property changes in CWEOE. Other future work
463 could include alternative narrow-band frequency binning and less strict auto-
464 mated rejection methods. Significant correlations across sets of consecutive (and
465 nearly consecutive) frequency bands indicate likely targets for potential follow-
466 up studies. Further development of a more complex classification scheme could
467 help improve the second tier discrimination of the proposed classifier, at the
468 level of discerning between the cognitive impairment types (e.g. mild/moderate

469 CI from severe CI). A thorough investigation into incorporating and comparing
470 additional classifiers is also a potential avenue for expansion of this research.

471 The NEUROPROFILE cohort was advantageous in that formal neuropsychological
472 testing was coupled with EEG recordings, making it ideal for this
473 investigation. However, there are study limitations. Although this novel study
474 used routine clinical EEGs used in the diagnosis of incidence cases of CWEOE,
475 the three classes of normal, mild/moderate and severe impairment were unbal-
476 anced; this occurred naturally. The majority of the sample was taken from a
477 population-based cohort, and mitigating potential influences from imbalanced
478 data was taken into account as much as possible when conducting the research,
479 e.g. through cost-sensitive analysis. Imbalanced data is not uncommon, but
480 the unbalanced distribution of CI in the current study reflects findings in a true
481 population-based cohort [45]. Furthermore, trialling this methodology in older
482 children with epilepsy may be an avenue for future studies, to provide further
483 insights as to the relationship between aetiology and CI, as well as provide
484 additional replications of the proposed techniques.

485 5. Limitations

486 Within the studied cohort of CWEOE, the epilepsy type and aetiologies were
487 heterogenous. Thus we are unable to determine if the model and methods used
488 have greater or lesser predictive value in specific subsets. Testing in a larger,
489 more homogeneous sample would provide clarification.

490 A gender disparity was noted within the normal cognition and mild/moderate
491 CI groups. Although this study reflects a true population, further studies are
492 needed to investigate this phenomena.

493 Note that the spectral components in the very low frequency narrow band
494 (e.g.1-3 Hz) may not be fully reliable due to the small epoch length, i.e. two
495 seconds. Information gained from the very low frequency band needs to be
496 interpreted with some care, as spurious connections are more likely to be present.
497 Again, however, the large number of trial epochs averaged for each child helped
498 mitigate these potential spurious connections.

499 We recognize a limitation in our assumption of dependency between the
500 frequency bins. While there is likely a strong local family dependency between
501 the narrow bins, the endpoints on our frequency spectrum may not have as
502 strong of a relation. Therefore, significance at these level should be considered
503 carefully as they are more likely to be a false positive. However, the robust
504 nature of τ and our choice of features from a machine-learning perspective help
505 to moderate potential impacts from this assumption on our results.

506 The use of a data-driven, narrow band approach in our analysis had a trade-
507 off of not using patient-specific frequency ranges for each child. Future studies
508 could be done to investigate how individualized frequencies, e.g. using individ-
509 ual alpha frequencies (IAF), could be aligned, interpreted and correlated when
510 assessing network abnormalities in the CWEOE population.

511 **6. Conclusions**

512 This study introduced a novel processing chain based on network analysis for
513 identifying markers of CI in CWEOE for the first time. Results from the study
514 demonstrate these network markers in identifying critical structures of CWEOE
515 with CI and illustrate their potential predictive abilities using preliminary clas-
516 sification techniques. Replication of the identified methods using other datasets,
517 with alternative narrow-band frequency binning, less strict automated rejection
518 methods, and including correlations with brain MRI abnormalities may bolster
519 the generalizability and applicability of the proposed techniques.

520 **7. Acknowledgements**

521 The authors would like to thank the patients and families who participated
522 in the NEUROPROFILES [45] study. Funding support for this project was
523 provided by the RS McDonald Trust, Thomas Theodore Scott Ingram Memorial
524 Fund, and the Muir Maxwell Trust.

525 **8. Author Contributions**

526 Javier Escudero and Richard FM Chin conceived of the presented ideas. Eli
527 Kinney-Lang developed the theory, performed data analysis and interpretation,
528 and designed the computational framework of the project under supervision
529 of Richard FM Chin and Javier Escudero. Jay Shetty, Krishnaraya Kamath
530 Tallur, Michael Yoong and Ailsa McLellan were involved in the methodology
531 and collection of the original NEUROPROFILES dataset, including recruiting
532 patients and requesting and reporting patient EEGs. Matthew Hunter was the
533 lead author and investigator for the NEUROPROFILES project with senior
534 supervision under Richard FM Chin. Eli Kinney-Lang wrote the manuscript
535 and figures, with revision and comments provided by Matthew Hunter, Michael
536 Yoong, Jay Shetty, Krishnaraya Kamath Tallur, Ailsa McLellan, Richard FM
537 Chin and Javier Escudero. Final approval of this publication was provided by
538 all authors.

539 **Conflict of Interest Statement**

540 None of the authors have potential conflicts of interest to be disclosed.

541 **References**

- 542 [1] B. S. Chang, D. H. Lowenstein, *Epilepsy*, *N. Engl. J. Med.* 349 (2003)
543 1257–1266. doi:10.1056/NEJMr022308.

- 544 [2] C. Reilly, P. Atkinson, K. B. Das, R. F. M. C. Chin, S. E. Aylett, V. Burch,
545 C. Gillberg, R. C. Scott, B. G. R. Neville, Neurobehavioral comorbidities in
546 children with active epilepsy: a population-based study., *Pediatrics* 133 (6)
547 (2014) e1586–93. doi:10.1542/peds.2013–3787.
548 URL <http://www.ncbi.nlm.nih.gov/pubmed/24864167>
- 549 [3] C. Reilly, P. Atkinson, K. B. Das, R. F. Chin, S. E. Aylett, V. Burch,
550 C. Gillberg, R. C. Scott, B. G. Neville, Factors associated with quality of
551 life in active childhood epilepsy: A population-based study, *Eur. J. Paedi-*
552 *atr. Neurol.* 19 (3) (2015) 308–313. doi:10.1016/J.EJPN.2014.12.022.
553 URL <https://www.sciencedirect.com/science/article/pii/S1090379815000069>
554
- 555 [4] E.-H. Kim, T.-S. Ko, Cognitive impairment in childhood onset epilepsy:
556 up-to-date information about its causes., *Korean J. Pediatr.* 59 (4) (2016)
557 155–64. doi:10.3345/kjp.2016.59.4.155.
558 URL <http://www.ncbi.nlm.nih.gov/pubmed/27186225><http://www.pubmedcentral.nih.gov/articlerender.fcgi?artid=PMC4865638>
559
- 560 [5] K. Rantanen, K. Eriksson, P. Nieminen, Cognitive impairment in preschool
561 children with epilepsy, *Epilepsia* 52 (8) (2011) 1499–1505. doi:10.1111/
562 *j.1528-1167.2011.03092.x*.
563 URL <http://doi.wiley.com/10.1111/j.1528-1167.2011.03092.x>
- 564 [6] D. B. Bailey, Critical thinking about critical periods (2001).
- 565 [7] W. A. Hauser, J. F. Annegers, W. A. Rocca, Descriptive Epidemiology of
566 Epilepsy: Contributions of Population-Based Studies From Rochester, Min-
567 nesota, *Mayo Clin. Proc.* 71 (6) (1996) 576–586. doi:10.4065/71.6.576.
568 URL <https://www.sciencedirect.com/science/article/pii/S0025619611641153><http://linkinghub.elsevier.com/retrieve/pii/S0025619611641153>
569
570
- 571 [8] B. Neville, Epilepsy in childhood., *BMJ Br. Med. J.* 315 (1997) 924–930.
572 URL <https://www.ncbi.nlm.nih.gov/pmc/articles/PMC2127609/pdf/9361544.pdf><http://www.ncbi.nlm.nih.gov/pmc/articles/PMC2127609/>
573
574
- 575 [9] M. J. England, C. T. Liverman, A. M. Schultz, L. M. Strawbridge, Epilepsy
576 across the spectrum: Promoting health and understanding. A summary of
577 the Institute of Medicine report (2012). doi:10.1016/j.yebeh.2012.06.
578 016.
- 579 [10] A. R. Brooks-Kayal, K. G. Bath, A. T. Berg, A. S. Galanopoulou, G. L.
580 Holmes, F. E. Jensen, A. M. Kanner, T. J. O’Brien, V. H. Whittemore,
581 M. R. Winawer, M. Patel, H. E. Scharfman, Issues related to symptomatic
582 and disease-modifying treatments affecting cognitive and neuropsychiatric
583 comorbidities of epilepsy, *Epilepsia* 54 (2013) 44–60. doi:10.1111/epi.

- 584 12298.
585 URL <http://doi.wiley.com/10.1111/epi.12298>
- 586 [11] M. Yoong, Quantifying the deficit-imaging neurobehavioural impairment
587 in childhood epilepsy., *Quant. Imaging Med. Surg.* 5 (2) (2015) 225–37.
588 doi:10.3978/j.issn.2223-4292.2015.01.06.
589 URL <http://www.ncbi.nlm.nih.gov/pubmed/25853081>[http://www.
590 pubmedcentral.nih.gov/articlerender.fcgi?artid=PMC4379313/
591 pmc/articles/PMC4379313/?report=abstract](http://www.pubmedcentral.nih.gov/articlerender.fcgi?artid=PMC4379313/pmc/articles/PMC4379313/?report=abstract)
- 592 [12] C. J. Stam, J. C. Reijneveld, Graph theoretical analysis of complex net-
593 works in the brain, *Nonlinear Biomed. Phys.* 1 (1) (2007) 3. doi:10.1186/
594 1753-4631-1-3.
595 URL [http://nonlinearbiomedphys.biomedcentral.com/articles/10.
596 1186/1753-4631-1-3](http://nonlinearbiomedphys.biomedcentral.com/articles/10.1186/1753-4631-1-3)
- 597 [13] E. Bullmore, O. Sporns, Complex brain networks: graph theoretical analy-
598 sis of structural and functional systems, *Nat. Rev. Neurosci.* 10 (4) (2009)
599 312–312. arXiv:arXiv:1011.1669v3, doi:10.1038/nrn2618.
600 URL <http://www.nature.com/doifinder/10.1038/nrn2618>
- 601 [14] C. J. Stam, Modern network science of neurological disorders, *Nat. Rev.*
602 *Neurosci.* 15 (10) (2014) 683–695. arXiv:arXiv:1011.1669v3, doi:10.
603 1038/nrn3801.
604 URL <http://www.nature.com/doifinder/10.1038/nrn3801>
- 605 [15] M. Yoong, M. Hunter, J. Stephen, A. Quigley, J. Jones, J. Shetty,
606 A. Mclellan, M. E. Bastin, R. F. M. Chin, Cognitive impairment in early
607 onset epilepsy is associated with reduced left thalamic volume, *Epilepsy*
608 *Behav.* doi:10.1016/j.yebeh.2018.01.018.
609 URL [https://www.epilepsybehavior.com/article/S1525-5050\(17\)
610 30945-9/pdf](https://www.epilepsybehavior.com/article/S1525-5050(17)30945-9/pdf)
- 611 [16] M. Friedman, The Use of Ranks to Avoid the Assumption of Normality
612 Implicit in the Analysis of Variance, *J. Am. Stat. Assoc.* 32 (200) (1937)
613 675. doi:10.2307/2279372.
614 URL <https://www.jstor.org/stable/2279372?origin=crossref>
- 615 [17] R. Oostenveld, P. Fries, E. Maris, J.-M. Schoffelen, FieldTrip: Open Source
616 Software for Advanced Analysis of MEG, EEG, and Invasive Electrophys-
617 iological Data, *Comput. Intell. Neurosci.* 2011 (2011) 1–9. arXiv:156869,
618 doi:10.1155/2011/156869.
619 URL <http://www.hindawi.com/journals/cin/2011/156869/>
- 620 [18] V. Miskovic, X. Ma, C.-A. Chou, M. Fan, M. Owens, H. Sayama, B. E.
621 Gibb, Developmental changes in spontaneous electrocortical activity and
622 network organization from early to late childhood., *Neuroimage* 118 (2015)
623 237–47. doi:10.1016/j.neuroimage.2015.06.013.
624 URL <http://linkinghub.elsevier.com/retrieve/pii/>

- 625 S1053811915005108[http://dx.doi.org/10.1016/j.neuroimage.](http://dx.doi.org/10.1016/j.neuroimage.2015.06.013)
626 2015.06.013[http://www.sciencedirect.com/science/article/](http://www.sciencedirect.com/science/article/pii/S1053811915005108)
627 pii/S1053811915005108[http://www.ncbi.nlm.nih.gov/pubmed/](http://www.ncbi.nlm.nih.gov/pubmed/26057595)
628 26057595<http://www.pubmedcentral.nih.go>
- 629 [19] G. Nolte, O. Bai, L. Wheaton, Z. Mari, S. Vorbach, M. Hallett, Identifying true brain interaction from EEG data using the imaginary part of coherency, *Clin. Neurophysiol.* 115 (10) (2004) 2292–2307. doi:10.1016/j.clinph.2004.04.029.
- 630
631
632
- 633 [20] G. Nolte, A. Ziehe, V. V. Nikulin, A. Schlögl, N. Krämer, T. Brismar, K.-R. Müller, Robustly Estimating the Flow Direction of Information in Complex Physical Systems, *Phys. Rev. Lett.* 100 (23) (2008) 234101. arXiv:0712.2352, doi:10.1103/PhysRevLett.100.234101.
634
635
636
637 URL <https://link.aps.org/doi/10.1103/PhysRevLett.100.234101>
- 638 [21] C. J. Stam, G. Nolte, A. Daffertshofer, Phase lag index: Assessment of functional connectivity from multi channel EEG and MEG with diminished bias from common sources, *Hum. Brain Mapp.* 28 (11) (2007) 1178–1193. doi:10.1002/hbm.20346.
639
640
641
- 642 [22] M. Vinck, R. Oostenveld, M. Van Wingerden, F. Battaglia, C. M. A. Pennartz, An improved index of phase-synchronization for electrophysiological data in the presence of volume-conduction, noise and sample-size bias, *Neuroimage* 55 (4) (2011) 1548–1565. arXiv:0006269v1, doi:10.1016/j.neuroimage.2011.01.055.
643
644
645
646
647 URL <http://dx.doi.org/10.1016/j.neuroimage.2011.01.055>
- 648 [23] S. Haufe, V. V. Nikulin, K.-R. Müller, G. Nolte, A critical assessment of connectivity measures for EEG data: A simulation study, *Neuroimage* 64 (1) (2013) 120–133. doi:10.1016/j.neuroimage.2012.09.036.
649
650
651 URL <http://dx.doi.org/10.1016/j.neuroimage.2012.09.036><http://linkinghub.elsevier.com/retrieve/pii/S1053811912009469>
652
- 653 [24] P. Tewarie, E. van Dellen, A. Hillebrand, C. J. Stam, The minimum spanning tree: An unbiased method for brain network analysis, *Neuroimage* 104 (2015) 177–188. doi:10.1016/j.neuroimage.2014.10.015.
654
655
656 URL <http://dx.doi.org/10.1016/j.neuroimage.2014.10.015>
- 657 [25] A. Fornito, A. Zalesky, E. T. Bullmore, Network scaling effects in graph analytic studies of human resting-state fMRI data, *Front. Syst. Neurosci.* 4 (2010) 22. doi:10.3389/fnsys.2010.00022.
658
659
660 URL [http://journal.frontiersin.org/article/10.3389/fnsys.](http://journal.frontiersin.org/article/10.3389/fnsys.2010.00022/abstract)
661 2010.00022/abstract
- 662 [26] B. C. M. Van Wijk, C. J. Stam, A. Daffertshofer, Comparing Brain Networks of Different Size and Connectivity Density Using Graph Theorydoi:10.1371/journal.pone.0013701.
663
664
665 URL <http://www.nwo.nl>

- 666 [27] K. Smith, H. Azami, M. A. Parra, J. M. Starr, J. Escudero, Cluster-span
667 threshold: An unbiased threshold for binarising weighted complete net-
668 works in functional connectivity analysis, Proc. Annu. Int. Conf. IEEE Eng.
669 Med. Biol. Soc. EMBS 2015-Novem (2015) 2840–2843. arXiv:1604.02403,
670 doi:10.1109/EMBC.2015.7318983.
- 671 [28] J. B. Kruskal, On the Shortest Spanning Subtree of a Graph and the
672 Traveling Salesman Problem, Proc. Am. Math. Soc. 7 (1) (1956) 48.
673 arXiv:arXiv:1011.1669v3, doi:10.2307/2033241.
674 URL [https://www.ams.org/journals/proc/1956-007-01/
675 S0002-9939-1956-0078686-7/S0002-9939-1956-0078686-7.pdf](https://www.ams.org/journals/proc/1956-007-01/S0002-9939-1956-0078686-7/S0002-9939-1956-0078686-7.pdf)<http://www.jstor.org/stable/2033241?origin=crossref>
676
- 677 [29] K. Smith, D. Abasolo, J. Escudero, Accounting for the complex hierarchical
678 topology of EEG phase-based functional connectivity in network binarisa-
679 tion, PLoS One.
- 680 [30] A. R. Gilpin, Table for Conversion of Kendall's Tau to Spearman's
681 Rho Within the Context of Measures of Magnitude of Effect for Meta-
682 Analysis, Educ. Psychol. Meas. 53 (1) (1993) 87–92. arXiv:0803973233,
683 doi:10.1177/0013164493053001007.
684 URL [http://epm.sagepub.com/cgi/doi/10.1177/
685 0013164493053001007](http://epm.sagepub.com/cgi/doi/10.1177/0013164493053001007)[http://journals.sagepub.com/doi/10.1177/
686 0013164493053001007](http://journals.sagepub.com/doi/10.1177/0013164493053001007)
- 687 [31] N. Shong, Pearson's versus Spearman's and Kendall's correlation coef-
688 ficients for continuous data, Ph.D. thesis (2010). arXiv:arXiv:1011.
689 1669v3, doi:10.1017/CB09781107415324.004.
- 690 [32] G. Fraga González, M. Van der Molen, G. Žarić, M. Bonte, J. Tijms,
691 L. Blomert, C. Stam, M. Van der Molen, Graph analysis of EEG resting
692 state functional networks in dyslexic readers, Clin. Neurophysiol. 127 (9)
693 (2016) 3165–3175. doi:10.1016/j.clinph.2016.06.023.
694 URL [http://linkinghub.elsevier.com/retrieve/pii/
695 S1388245716304539](http://linkinghub.elsevier.com/retrieve/pii/S1388245716304539)
- 696 [33] M. Hall, E. Frank, G. Holmes, B. Pfahringer, P. Reutemann, I. H. Witten,
697 The WEKA data mining software, ACM SIGKDD Explor. 11 (1) (2009)
698 10–18. doi:10.1145/1656274.1656278.
699 URL [http://portal.acm.org/citation.cfm?doid=1656274.1656278&
700 delimiter=026E30F&npapers2://publication/doi/10.1145/1656274.
701 1656278](http://portal.acm.org/citation.cfm?doid=1656274.1656278&delimiter=026E30F&npapers2://publication/doi/10.1145/1656274.1656278)
- 702 [34] E. Frank, M. A. Hall, I. H. Witten, The WEKA Workbench, in: Morgan
703 Kaufmann, Fourth Ed., Elsevier, 2016, pp. 553–571.
704 URL [http://www.cs.waikato.ac.nz/ml/weka/
705 Witten%20et%20al%202016%20appendix.pdf](http://www.cs.waikato.ac.nz/ml/weka/Witten%20et%20al%202016%20appendix.pdf)

- 706 [35] S. Khalid, T. Khalil, S. Nasreen, A survey of feature selection and feature
707 extraction techniques in machine learning, in: 2014 Sci. Inf. Conf., IEEE,
708 2014, pp. 372–378. doi:10.1109/SAI.2014.6918213.
709 URL [http://ieeexplore.ieee.org/lpdocs/epic03/wrapper.htm?](http://ieeexplore.ieee.org/lpdocs/epic03/wrapper.htm?arnumber=6918213)
710 [arnumber=6918213](http://ieeexplore.ieee.org/lpdocs/epic03/wrapper.htm?arnumber=6918213)
- 711 [36] Z.-H. Zhou, X.-Y. Liu, On multi-class cost-sensitive learning, *Comput.*
712 *Intell.* 26 (3) (2010) 232–257. doi:10.1111/j.1467-8640.2010.00358.x.
713 URL [https://www.scopus.com/inward/record.uri?eid=2-s2.](https://www.scopus.com/inward/record.uri?eid=2-s2.0-77955034751&doi=10.1111%7D2fj.1467-8640.2010.00358.x&partnerID=40&md5=21d7f85735dd6b67beeb0f73e6177cf7)
714 [0-77955034751{&}doi=10.1111{%}2fj.1467-8640.2010.00358.](https://www.scopus.com/inward/record.uri?eid=2-s2.0-77955034751&doi=10.1111%7D2fj.1467-8640.2010.00358.x&partnerID=40&md5=21d7f85735dd6b67beeb0f73e6177cf7)
715 [x{&}partnerID=40{&}md5=21d7f85735dd6b67beeb0f73e6177cf7](https://www.scopus.com/inward/record.uri?eid=2-s2.0-77955034751&doi=10.1111%7D2fj.1467-8640.2010.00358.x&partnerID=40&md5=21d7f85735dd6b67beeb0f73e6177cf7)
- 716 [37] J. Shao, Bootstrap Model Selection, *J. Am. Stat. Assoc.* 91 (434) (1996)
717 655–665. doi:10.2307/2291661.
718 URL [http://www.jstor.org/stable/2291661\\$\\](http://www.jstor.org/stable/2291661$\\delimitter)
719 [delimitter"026E30F\\$nhhttps://www.jstor.org/stable/pdfplus/10.](http://www.jstor.org/stable/2291661$\\delimitter)
720 [2307/2291661.pdf?acceptTC=true](http://www.jstor.org/stable/2291661$\\delimitter)
- 721 [38] P. J. Marshall, Y. Bar-Haim, N. A. Fox, Development of the EEG from 5
722 months to 4 years of age, *Clin. Neurophysiol.* 113 (8) (2002) 1199–1208.
723 doi:10.1016/S1388-2457(02)00163-3.
724 URL [http://www.sciencedirect.com/science/article/pii/](http://www.sciencedirect.com/science/article/pii/S1388245702001633)
725 [S1388245702001633](http://www.sciencedirect.com/science/article/pii/S1388245702001633)
- 726 [39] E. OREKHOVA, T. STROGANOVA, I. POSIKERA, M. ELAM, EEG
727 theta rhythm in infants and preschool children, *Clin. Neurophysiol.* 117 (5)
728 (2006) 1047–1062. doi:10.1016/j.clinph.2005.12.027.
729 URL [http://linkinghub.elsevier.com/retrieve/pii/](http://linkinghub.elsevier.com/retrieve/pii/S1388245706000095)
730 [S1388245706000095](http://linkinghub.elsevier.com/retrieve/pii/S1388245706000095)
- 731 [40] A. Chiang, C. Rennie, P. Robinson, S. van Albada, C. Kerr, Age trends and
732 sex differences of alpha rhythms including split alpha peaks, *Clin. Neuro-*
733 *physiol.* 122 (8) (2011) 1505–1517. doi:10.1016/j.clinph.2011.01.040.
734 URL [http://linkinghub.elsevier.com/retrieve/pii/](http://linkinghub.elsevier.com/retrieve/pii/S1388245711000903)
735 [S1388245711000903](http://linkinghub.elsevier.com/retrieve/pii/S1388245711000903)
- 736 [41] T. a. B. Snijders, The degree variance: An index of graph heterogeneity,
737 *Soc. Networks* 3 (3) (1981) 163–174. doi:10.1016/0378-8733(81)
738 90014-9.
739 URL [http://linkinghub.elsevier.com/retrieve/pii/](http://linkinghub.elsevier.com/retrieve/pii/0378873381900149)
740 [0378873381900149](http://linkinghub.elsevier.com/retrieve/pii/0378873381900149)
- 741 [42] M. Matsuura, K. Yamamoto, H. Fukuzawa, Y. Okubo, H. Uesugi, M. Mori-
742 iwa, T. Kojima, Y. Shimazono, Age development and sex differences of
743 various EEG elements in healthy children and adults—quantification by a
744 computerized wave form recognition method, *Electroencephalogr Clin Neu-*
745 *rophysiol* 60 (5) (1985) 394–406. doi:10.1016/0013-4694(85)91013-2.
746 URL <http://www.ncbi.nlm.nih.gov/pubmed/2580690>

- 747 [43] A. Amador, P. Valdés Sosa, R. Pascual Marqui, L. Garcia, R. Lirio, J. Ba-
748 yard, On the structure of EEG development, *Electroencephalogr. Clin.*
749 *Neurophysiol.* 73 (1) (1989) 10–19. doi:10.1016/0013-4694(89)90015-1.
750 URL [http://linkinghub.elsevier.com/retrieve/pii/](http://linkinghub.elsevier.com/retrieve/pii/0013469489900151)
751 [0013469489900151](http://linkinghub.elsevier.com/retrieve/pii/0013469489900151)
- 752 [44] T. Gasser, R. Verleger, P. Bächer, L. Sroka, Development of the
753 EEG of school-age children and adolescents. I. Analysis of band
754 power, *Electroencephalogr. Clin. Neurophysiol.* 69 (2) (1988) 91–99.
755 doi:10.1016/0013-4694(88)90204-0.
756 URL [http://linkinghub.elsevier.com/retrieve/pii/](http://linkinghub.elsevier.com/retrieve/pii/0013469488902040)
757 [0013469488902040](http://linkinghub.elsevier.com/retrieve/pii/0013469488902040)
- 758 [45] H. M.B., S. R., V. K., Y. M., M. A., S. J., C. R.F., NEUROde-
759 velopment in PReschool Children Of Fife and Lothian Epilepsy
760 Study: NEUROPROFILES - A population-based study (2015).
761 doi:<http://dx.doi.org/10.1111/epi.12675>.
762 URL [http://ovidsp.ovid.com/ovidweb.cgi?T=JS{&}PAGE=](http://ovidsp.ovid.com/ovidweb.cgi?T=JS{&}PAGE=reference{&}D=emed12{&}NEWS=N{&}AN=71754114)
763 [reference{&}D=emed12{&}NEWS=N{&}AN=71754114](http://ovidsp.ovid.com/ovidweb.cgi?T=JS{&}PAGE=reference{&}D=emed12{&}NEWS=N{&}AN=71754114)
- 764 [46] C. J. Stam, Nonlinear dynamical analysis of EEG and MEG: Review of an
765 emerging field (oct 2005). doi:10.1016/j.clinph.2005.06.011.
766 URL [http://linkinghub.elsevier.com/retrieve/pii/](http://linkinghub.elsevier.com/retrieve/pii/S1388245705002403)
767 [S1388245705002403](http://linkinghub.elsevier.com/retrieve/pii/S1388245705002403)
- 768 [47] J. Cabral, M. L. Kringelbach, G. Deco, Exploring the network dynamics
769 underlying brain activity during rest, *Prog. Neurobiol.* 114 (2014) 102–131.
770 doi:10.1016/j.pneurobio.2013.12.005.
771 URL <http://dx.doi.org/10.1016/j.pneurobio.2013.12.005>
- 772 [48] M.-T. Horstmann, S. Bialonski, N. Noennig, H. Mai, J. Prusseit,
773 J. Wellmer, H. Hinrichs, K. Lehnertz, State dependent properties of epilep-
774 tic brain networks: comparative graph-theoretical analyses of simultane-
775 ously recorded EEG and MEG., *Clin. Neurophysiol.* 121 (2) (2010) 172–85.
776 doi:10.1016/j.clinph.2009.10.013.
777 URL <http://www.ncbi.nlm.nih.gov/pubmed/20045375>
- 778 [49] P. L. Nunez, R. Srinivasan, A. F. Westdorp, R. S. Wijesinghe, D. M.
779 Tucker, R. B. Silberstein, P. J. Cadusch, EEG coherency I: Statistics,
780 reference electrode, volume conduction, Laplacians, cortical imag-
781 ing, and interpretation at multiple scales 103 (5) (1997) 499–515.
782 doi:10.1016/S0013-4694(97)00066-7.
783 URL [http://linkinghub.elsevier.com/retrieve/pii/](http://linkinghub.elsevier.com/retrieve/pii/S0013469497000667)
784 [S0013469497000667](http://linkinghub.elsevier.com/retrieve/pii/S0013469497000667)

785 **Appendix A. Network Coupling Definitions**

786 Appendix A outlines the key network definitions and details for the presented
787 analysis. For in-depth reviews see [46, 13], and for further reading [12, 47, 48].

788 *Cross-spectrum*

Functional EEG connections are established through measures of interdependency between signals s_i and s_j [48] for any pair of EEG channels i and j . A common measurement for examining this interdependency is the cross-spectrum function $S_{ij}(f)$ [49, 19, 48]. Formally, let $x_i(f)$ and $x_j(f)$ be the complex Fourier transforms of the time series signals s_i and s_j for any pair (i, j) of EEG channels. Then the cross-spectrum can be calculated as

$$S_{ij}(f) \equiv \langle x_i(f)x_j^\dagger(f) \rangle \quad (\text{A.1})$$

789 where \dagger indicates the complex conjugation, and $\langle \rangle$ refers to the expectation value
790 (also written as $E\{\}$) [19].

791 *Imaginary Part of Coherency (ICOH)*

Coherency is defined as the normalized cross-spectrum[19]:

$$C_{ij}(f) \equiv \frac{S_{ij}(f)}{(S_{ii}(f)S_{jj}(f))^{1/2}} \quad (\text{A.2})$$

Therefore, the imaginary part of coherency is defined as [19]

$$ICoh_{ij}(f) \equiv Im\{C_{ij}(f)\} \quad (\text{A.3})$$

792 where $Im\{\}$ refers to taking the imaginary part of the complex coherency mea-
793 sure.

794 *Phase-Slope Index (PSI)*

The PSI is defined as:

$$\Psi_{ij}(f) = Im\left\{\sum_{f \in F} C_{ij}^\dagger(f)C_{ij}(f + \delta f)\right\} \quad (\text{A.4})$$

795 where $C_{ij}(f)$ is as defined in equation A.2, \dagger indicates the complex conjugation,
796 δf is the frequency resolution, and $f \in F$ is the set of frequencies over which
797 the phase-slope is calculated (see [20] for details).

798 *Phase-Lag Index*

The PLI is defined as: [21, 22]

$$\Theta_{ij} \equiv |E\{sign(Im\{C_{ij}(f)\})\}| \quad (\text{A.5})$$

799 where $E\{\}$ is the expectation, $sign$ is the positive or negative sign, and $Im\{C_{ij}(f)\}$
800 is the same as ICOH (see equation A.3).

801 *Weighted Phase-Lag Index (WPLI)*

The weighted PLI (WPLI) is defined as: [22]

$$\Phi_{ij}(f) \equiv \frac{|E\{|Im\{X\}|sign(Im\{X\})\}|}{E\{|Im\{X\}|} \quad (\text{A.6})$$

802 where $X = Im\{C_{ij}(f)\} = ICoh_{ij}(f)$.

803 **Appendix B. Supplementary Figures**

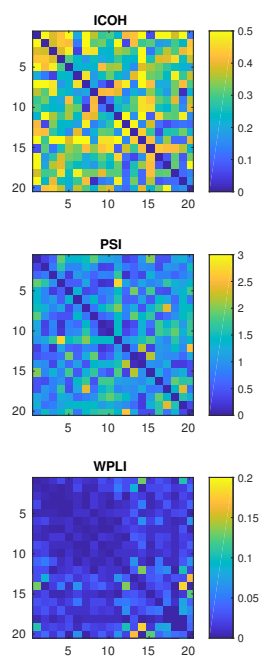


Figure B.5: Adjacency matrices for a representative 'normal cognition' child calculated by ICOH, PSI and WPLI between the 5-9 Hz frequency range.

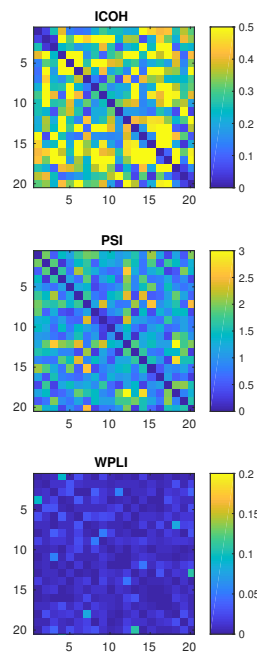


Figure B.6: Adjacency matrices for a representative 'impaired cognition' child calculated by ICOH, PSI and WPLI between the 5-9 Hz frequency range.